Improving the interpretation of diffusional kurtosis by resolving effects of isotropic and anisotropic microstructures

Filip Szczepankiewicz[1], Danielle van Westen[2,3], Jimmy Lätt[2], Elisabet Englund[3], Carl-Fredrik Westin[4], Freddy Ståhlberg[1,3], Pia C. Sundgren[2,3], and Markus Nilsson[5]
[1]*Dept. of Medical Radiation Physics, Lund University, Lund, Sweden,* [2]*Imaging and Function, Skåne University Healthcare, Lund, Sweden,* [3]*Dept. of Clinical Sciences, Lund University, Skåne University Healthcare, Lund, Sweden,* [4]*Dept. of Radiology, Brigham and Women's Hospital, Harvard Medical School, Boston, MA, United States,* [5]*Lund University Bioimaging Center, Lund University, Lund, Sweden*

Introduction – Diffusional kurtosis imaging (DKI) is useful for investigating tissue microstructure [1, 2], however, interpreting kurtosis parameters is challenging because conventional methods cannot distinguish between the mechanisms that give rise to the kurtosity. In this work, we use conventional and single-shot isotropic diffusion encoding to separate kurtosity into contributions from isotropic and anisotropic microstructure. We demonstrate this method in glioma and meningioma tumors in vivo, and show that the kurtosity observed in the two tumors originates from different microstructural features.

Theory – For conventional (directional) diffusion encoding at moderate encoding strength ($b < 3$ ms/μm^2), the MR signal, S(b), is determined only by the expectancy and variance of the underlying distribution of diffusion coefficients, P(D) [3]. Thus, diffusional kurtosis caused by radically different microstructural features can appear identical when using methods based on conventional encoding, such as DKI.

We illustrate this problem by comparing two microstructure models inspired by malignant glioma (G) and meningioma (M) histology (Fig. 1). In the glioma, P(D) reflects the presence of isotropic domains with varying domain mean diffusivities; and in the meningioma, P(D) reflects the presence of randomly oriented anisotropic domains. For these two distributions, with equal expectancy and variance, the S(b) is virtually identical for the two models (Fig. 1), and cannot be distinguished. However, by using single-shot isotropic encoding, the influence of diffusion anisotropy is removed, and the signal is made sensitive only to the mean diffusivity of the underlying domains [4, 5]. Isotropic encoding can thus be used to distinguish between the two microstructure models, since the distribution of domain mean diffusivities is wide for the glioma model, but very narrow for the meningioma model.

Methods – Eleven patients, 5 with malignant glioma (high grade) and 6 with meningioma (low grade), were scanned using a Philips Achieva 3T system equipped with an 80 mT/m gradient system. Informed written consent was obtained prior to scanning. Data was acquired using directional and single-shot isotropic encoding. The latter was achieved by spinning the q-vector at the magic angle (qMAS) [5]. Images were acquired in five axial slices, centered on the lesion in each patient, at a spatial resolution of 3×3×3 mm^3. Both encoding techniques employed ten equidistant b-values between 100 and 2800 s/mm^2, TE = 160 ms, and TR = 2000 ms. The total acquisition time was 10 min.

The total kurtosis, corresponding to the mean apparent diffusional kurtosis measured with DKI, was defined as $K_T = V_T / MD^2$, where V_T is the variance of P(D), and MD is the mean diffusivity. K_T was estimated by fitting the Laplace transform of the gamma distribution function to the powder average of the data acquired using directional encoding [4, 5]. The isotropic component, K_I, was estimated based on data acquired using isotropic encoding. The anisotropic component, K_A, was calculated according to $K_A = K_T - K_I$ [4]. Finally, K_A was also expressed in terms of the microscopic fractional anisotropy, $\mu FA = (2/3 + 4/15/K_A)^{-1/2}$ [5]. The μFA was calculated to provide another interpretation of K_A, since μFA represents the FA that would be observed if the domains in each voxel were perfectly aligned [4, 5].

Tumor ROIs were manually defined in each patient, avoiding edema and healthy tissue. Rank-sum tests were performed to test median difference, with respect to K_T, K_A, K_I, and μFA, between the glioma and meningioma groups (* denotes $p < 0.05/4$, Bonferroni corrected).

Results – Figure 2 shows morphological images and the kurtosis maps for two representative patients. Figure 3 shows a group comparison across all kurtosis components between the gliomas and meningiomas. The total kurtosity in the gliomas was almost solely explained by variance in the domain mean diffusivity ($K_T \approx K_I$, and $K_A \approx 0$), while in the meningiomas, it was predominately explained by the presence of anisotropic micro-domains ($K_A > K_I$). Compared to the gliomas, the meningiomas exhibited significantly higher K_T. The gliomas exhibited a slightly higher K_I, but not with significance. Most prominently, the meningiomas had a significantly higher K_A, and consequently also higher μFA, compared to the gliomas, which indicates anisotropic microstructure in the meningiomas.

Discussion and Conclusions – In this study, diffusional kurtosis was investigated in two tumor types with radically different microstructures. The gliomas exhibited low levels of microscopic anisotropy ($K_A \approx 0$) and a higher level of isotropic heterogeneity. The low values of K_A indicate isotropic cell structures in the gliomas, and the elevated K_I may be due to heterogeneous cell sizes or partial volume effects from free water in necrotic parts of the tumor. By contrast, the dominant part of the kurtosis in the meningiomas was due to the presence of microscopic anisotropy, probably caused by the randomly oriented eccentric cells within the tissue [4]. Separating the kurtosis into its components yields a more powerful statistical separation between groups (Fig. 3). Quantification of K_A allows the diffusional kurtosity to be interpreted in terms of μFA, i.e., the FA value that would have been obtained if all cells were parallel.

In conclusion, conventional DKI is sensitive to the total diffusional kurtosis, but is not specific in regard to the microstructural features that cause the kurtosity. By extending the conventional DKI acquisition scheme with single-shot isotropic encoding, it is possible to resolve the contributions from the presence of domains with varying isotropic diffusivities, and the presence of microscopic anisotropy. When investigated separately, each component may provide more specific information, which improves the interpretation of diffusional kurtosis parameters and their relationship to the microstructure.

References – [1] Jensen et al. 2005, MRM 53:1432-40; [2] Steven et al. 2014, AJR 202; [3] Mitra 1995, Phys Rev B 51; [4] Szczepankiewicz et al. 2014, Neuroimage 104:241-52; [5] Lasič et al. 2014, FPHY 2

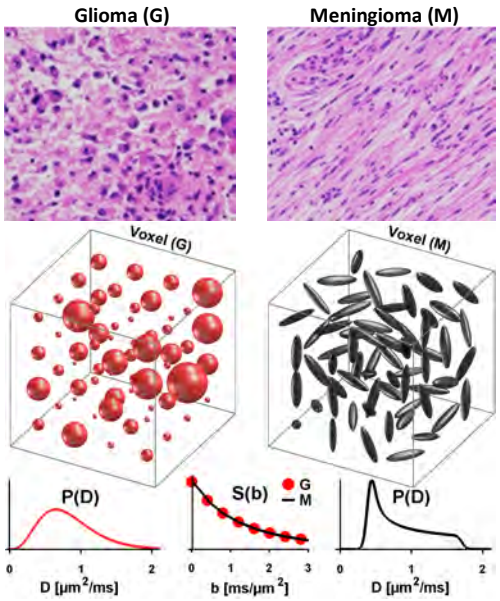

Figure 1 – Representative histology (top row), microstructure models of glioma and meningioma (middle row). We approximate the glioma microstructure by domains with isotropic diffusion and varying diffusivity, and the meningioma by randomly oriented domains with anisotropic diffusion. By design, both microstructures exhibit distributions of diffusion coefficients that have the same mean diffusivity and variance which renders identical signal in conventional diffusion experiments (bottom row).

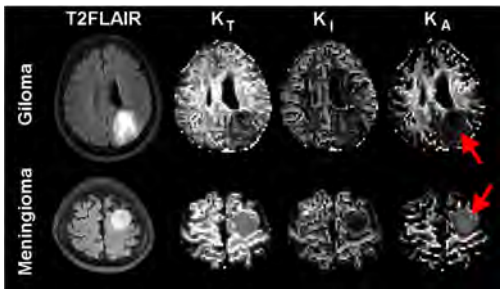

Figure 2 – Morphology and kurtosis in glioma (top row) and meningioma (bottom row). The meningioma exhibited a prominent anisotropic kurtosis while the glioma did not (red arrows). Isotropic kurtosis was approximately equal. The windowing was identical in all kurtosis maps.

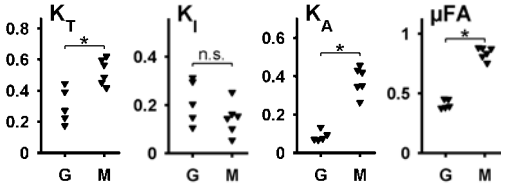

Figure 3 – Comparison of average values in the two tumor types. The total kurtosis was higher in the meningioma. Both tumor types had similar isotropic kurtosis. Most notably, the anisotropic kurtosis and μFA was markedly higher in the meningiomas, in agreement with expectations from histology.